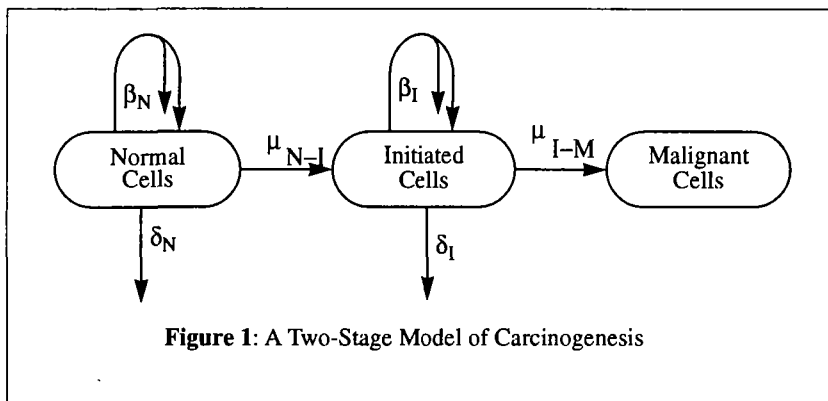


A Biologically-Based Model for the Carcinogenic Effects of 2,3,7,8-TCDD in Female Sprague-Dawley Rats

C. Portier and M. Kohn

Laboratory of Computational Biological and Risk Analysis, National Institute of Environmental Health Sciences, Research Triangle Park, North Carolina, USA 27709

1.0 Introduction. In recent years, there has been a resurgence in interest in refining the mechanistic representation of mathematical models of carcinogenesis. With few exceptions, the mathematical modeling of carcinogenesis at the cellular level has relied on the use of the multistage model. Theoretical discussions on these models began in the mid-20th century. One major failure of the early models was a lack of growth kinetics of the cell populations; this was relaxed by several authors who proposed the two-stage model, which is illustrated in Figure 1.



The two-stage model assumes that carcinogenesis is the result of two critical mutations, the first resulting in an intermediate cell population and the second resulting in malignancy. The number of cells in the normal and intermediate populations are allowed to increase in number via replication or reduce in number due to death or differentiation. There are different mathematical approaches to this model since several groups have proposed the same model but used different mathematical developments to predict tumor incidence from this model. In the application of the two-stage model that follows, the mathematical development of this model by Moolgavkar and Venzon (1) and the subsequent development of this form of the stochastic process will be used.

The two-stage model has six basic rates that must be estimated. These are:

- β_N = birth rate for cells in the normal state.
- δ_N = death/differentiation rate for cells in the normal state.
- μ_{N-I} = rate at which mutations occur adding cells to the intermediate state.
- β_I = birth rate for cells in the intermediate state.
- δ_I = death rate for cells in the intermediate state.
- μ_{I-M} = rate at which mutations occur adding cells to the malignant state.

To apply this model to dioxin, or any other chemical carcinogen, requires estimates of these rates as they change over dose and time. A mechanistic approach would incorporate changes in biomarker proteins estimated by a biochemical model directly into the two-stage model as rate changes in these parameters. Portier et al. (2) developed methods for modeling in this manner.

In addition, it is possible to apply this model to premalignant focal lesions in the liver in order to estimate μ_{N-I} , β_I and δ_I . One problem with this latter approach is that it is currently limited to a relatively small number of changes in the parameters over time (piecewise constant process), which makes it difficult to link the method to biochemical models. However, restricting the analysis to constant rates, it is possible to combine these models with tumor incidence data to predict overall carcinogenicity. There is one applicable analysis of liver focal lesion data in female Sprague-Dawley rats available for this exercise (3) and one analysis in Wistar rats (4). Finally, there is no published method available for linking tumor incidence data, focal lesion data and biochemical models which will utilize nonhomogeneous rates in the model

The liver tumor responses from the Kociba et al. (5) study are given in Table 1 using the most recent pathology review of the liver sections (6). Shown are the number of animals with tumor (row 2), number of animals placed on study (row 3), a survival-adjusted number of animals at risk (row 4), and the survival-adjusted lifetime tumor probability (row 5 which equals the entry in row 2 divided by the entry in row 4).

Table 1: Liver tumors in female Sprague-Dawley rats from the study of Kociba et al. (5) using the recent pathology (6)

	Control	1 ng/kg/day	10 ng/kg/day	100 ng/kg/day
# With Tumor	2	1	9	18
# Initially on Study	86	50	50	50
Survival-Adjusted # at Risk	57	34	27	31
Lifetime Tumor Risk	0.035	0.029	0.333	0.581

2. Mechanistic models involving hepatic focal lesions. It has been suggested that clones of cells which express one of several biochemical alterations (hepatic focal lesions) correspond to the initiated cells in the two-stage model of carcinogenesis. Two data sets (7,8) exist in the literature with sufficient information on dose-response to allow for modeling the effect of dose on the rates in the first half of the two-stage model shown in Figure 1. Portier et al. (3) analyzed the data in (7) and esti-

mated the effect of dose on μ_{N-I} , β_I and δ_I .

Portier et al. (3) estimated the parameters in the first half of the two-stage mathematical model of carcinogenesis from these data. Their results suggest that TCDD stimulates the production of PGST+ foci (a mutational effect) and promotes the growth of PGST+ foci (a birth rate effect). Data on cell labeling and on liver weight could not explain the mutational effect of TCDD. Following upon the work of Kohn et al. (9), Portier et al. suggested this finding could be due to an increase in the metabolism of estrogens to catechol estrogens leading to subsequent increase in free oxygen radicals and eventually to mutations. This finding indicates a complicated mechanism for TCDD-induced production of hepatic foci that they refer to as activation, labelling TCDD as an activator.

As a validation exercise, they used the same methods to analyze data from Pitot et al. (8). Portier et al. found that all four lesions from the two different studies produced similar qualitative results; dioxin had both a promotion effect and an activation effect. The effect of dose on the birth rates (β_I) for both data sets were shown to produce similar patterns with an almost identical unexposed birth rate for all of the four lesion types; a maximal increase over the background rate of 33-300%, saturation of the increased birth rate at low doses and a small increase in birth rate due to DEN initiation. The pattern of dose-related changes in the mutation rate (μ_{N-I}) response is slightly different in ATP, GGT and G6P foci than for the PGST+ foci; tending more toward linearity than the hyperbolic response seen for the PGST+ foci. However, for all four lesions, the maximal induction rate tended to be the same.

Moolgavkar et al. (4) analyzed data from Buchmann et al. (10) on ATP foci in female Wistar rats exposed to 2,3,7,8-TCDD as well as 1,2,3,4,6,7,8-heptachlorodibenzo-p-dioxin. In addition to the mathematical analysis used by Portier et al. (3) (which was developed by Moolgavkar and colleagues), Moolgavkar et al. used a modification which allowed for cellular proliferation focused on the edge of the ATP foci. While they did not have information on multiple dose groups, the results of their analysis for TCDD concur qualitatively with those of Portier et al. (3). In essence, they observed a moderate effect (approximately a 25% increase) of TCDD on the birth rate of initiated cells (β_I), a significant (10x in non-initiated and 2x in initiated) effect of TCDD on μ_{N-I} and a prolonged effect of DEN following initiation (similar to the interaction effect observed by 3). The observed change in birth rates is quantitatively similar to that observed by Portier et al. for PGST+, GGT and G6P foci but smaller than that for ATP foci. In the DEN initiated groups, the associated increases in the mutation rates were quantitatively similar to those observed for PGST+ lesions in the Portier et al. study (2.2 x at 100 ng/kg/day in Moolgavkar et al., 2.5 at 125 ng/kg/day for PGST+), but much smaller than that observed for the ATP, GGT and G6P lesions from the Pitot et al. study (9.9x for ATP, 4.5x for GGT and 5.8x for G6P). The observed increase in μ_{N-I} in non-initiated animals was much larger in the Moolgavkar et al. analysis than that for the Portier et al. analysis.

As mentioned earlier, these analyses have either been done with constant rates or few piecewise-constant rates and the methods do not lend themselves to continuous changes in the parameters over time. However, the analyses do suggest that any model developed for the carcinogenicity of dioxin should include treatment/exposure related effects on both the mutation rates and the birth rates. These concepts will be developed in the next section.

3. Mechanistic models for carcinogenesis. Kohn et al. (9) hypothesized that induction of CYP1A2 could lead to an increase in the metabolism of estrogens to catechol estrogens and that further activation of these catechol estrogens can lead to oxidative DNA damage and eventually to mutations. Thus, the instantaneous concentration of CYP1A2 could serve as a useful dose surrogate for the mutational effects (μ_{N-I}) of TCDD expressed in the two-stage model shown in Figure 1. Kohn et al. (9) also provided a potential mechanism for the proliferative effects of TCDD on the cells in the intermediate state. For this process, they propose a mechanism based on the incorporation of the

EGF receptor in an activated state in the cell interior rather than on the cellular membrane. Thus, instantaneous concentration of the amount of activated EGF receptor would serve as a useful biomarker of dose-related changes in the birth rate (β_1) in the two-stage model.

Portier et al. (1996) provide a means for calculating tumor incidence for any multistage model including those with time-varying rates. By simply linking the calculated tumor incidence function with an appropriate likelihood for the tumor of interest, estimates of the model parameters can be obtained by maximizing the likelihood.

The simplest two-stage model one could fit to the tumor data and remain consistent with the promotion and oxidative damage mechanisms is one in which $\beta_N(t,d)=\delta_N(t,d)=0$, $\mu_{N1}(t,d)=a_1C_2(t,d)$, $\beta_1(t,d)=a_2+a_3E(t,d)$, $d_1(t,d)=a_4E(t,d)$ and $\mu_{1M}(t,d)=a_5$ where $C_2(t,d)$ is the concentration of CYP1A2 at time t given dose d, $E(t,d)$ is the concentration of activated EGF receptor at time t given dose d and a_1 to a_5 are parameters which must be estimated. The functions C_2 and E are available from the model of Kohn et al. (9) by simulating the model using input parameters appropriate for the cancer study. The estimated model parameters are given in Table 2.

Table 2: Parameter estimates derived for fitting the tumor incidence counts of (6) using the dose surrogates of Kohn et al. (9) and a two-stage model

Parameter	Units	Estimate (95% Confidence Interval)
a1	mutations/cell/day/nmol CYP1A2/g liver	4.2x10 ⁻¹¹ (3.98 x10 ⁻¹¹ ,4.36 x10 ⁻¹¹)
a2	births/cell/day	8.32x10 ⁻³ (5.30 x10 ⁻³ ,13.1 x10 ⁻³)
a3	births/cell/day/nmol EGFR/g liver	1.86x10 ⁻⁵ (0.76 x10 ⁻⁵ ,4.59 x10 ⁻⁵)
a4	deaths/cell/day/nmol EGFR/g liver	5.73x10 ⁻² (5.48 x10 ⁻² ,5.99 x10 ⁻²)
a5	mutations/cell/day	2.64x10 ⁻⁵ (2.52 x10 ⁻⁵ ,2.76 x10 ⁻⁵)

The fit of the model to the survival-adjusted lifetime tumor-prevalence is given in Table 3. All of the predictions lie within the range of the data, but are a bit high for the lowest dose group and the highest dose group. This is predominantly due to most of the tumors arising very late in the experiment (17 of the 31 tumors were observed after 705 days with the remaining 14 all in the highest dose group).

Table 3: Observed lifetime tumor probability (95% confidence interval) compared to predicted risk from the two-stage model

Dose	0 ng/kg/day	1 ng/kg/day	10 ng/kg/day	100 ng/kg/day
Survival-Adjusted Tumor Risk	0.035 (0.0,0.12)	0.029 (0.0,0.12)	0.333 (0.13,0.42)	0.581 (0.42,0.73)
Predicted Risk	0.044	0.123	0.284	0.712

TOX III

This model can be used to estimate low dose risks for TCDD or benchmark doses. Point estimates for various risks are provided in Table 4. The larger excess risk numbers (0.001-0.05) can be used for benchmark dose risk estimation and the remaining value (10^{-6}) is the dose yielding 1 excess tumor per million at risk. It is clear from the pattern of response seen in Table 4 that, in the low-dose range, risk is proportional to dose. This follows from the findings in the model by Kohn et al. in which all Hill coefficients for the important quantities were estimated to be approximately 1. As Portier et al. (11) point out, this results in linear behavior in the low-dose range.

Table 4: Doses yielding specified excess risks for female rats exposed to TCDD

Excess Risk	0.05	0.01	0.005	0.001	1×10^{-6}
Pred. Dose (ng/kg/day)	6.50×10^{-1}	1.46×10^{-1}	7.40×10^{-2}	1.44×10^{-2}	1.50×10^{-5}

4. Adequacy of the Two-Stage Model for Risk Assessment. Some of the mechanistic assumptions in this model are speculative. The two-stage model of carcinogenesis used in this analysis has encoded the transformation of cells from a normal state to a malignant state as mathematical equations based upon the assumptions such as cell independence. The exact nature of these transformations are unknown and could conceivably have an impact on the predictions from the model. The linkage between the PBPK model of Kohn et al. and the two-stage model is also speculative and, undoubtedly, impacts upon the risk projections.

It should be noted that the mechanistic models can suggest experimental strategies for testing hypotheses regarding the mechanism of action of TCDD and validating these models. For the purposes of risk estimation, one must be careful to recognize that these models do not necessarily impart added confidence in low-dose risk estimates, because the mechanistic links between TCDD-mediated changes in gene expression and toxic responses are not completely known.

5. References.

1. Moolgavkar, S. and Venzon, D. Two-event models for carcinogenesis: Incidence curves for childhood and adult tumors. *Mathematical Biosciences* **47**, 55-77. 1979.
2. Portier, C., Kopp-Schneider, A. and Sherman, C. Calculating tumor incidence rates in stochastic models of carcinogenesis. *Mathematical Biosciences* (in press). 1996.
3. Portier, C.J., Kohn, M.C., Kopp-Schneider, A., Sherman, C.D., Maronpot, R., and Lucier, G.W. Modeling the number and size of hepatic focal lesions following exposure to 2,3,7,8-TCDD. *Toxicology and Applied Pharmacology* **137**, (in press) 1996.
4. Moolgavkar, S., Luebeck, E., Buchmann, A. and Bock, K. Quantitative analysis of enzyme-altered liver foci in rats initiated with diethylnitrosamine and promoted with 2,3,7,8-tetrachlorodibenzo-p-dioxin or 1,2,3,4,6,7,8-heptachlorodibenzo-p-dioxin. *Toxicology and Applied Pharmacology* **138**, (in press). 1996.
5. Kociba, R. J., Keyes, D. G., Beyer, J., et al. Results of a two year chronic toxicity and oncogenicity study of 2,3,7,8-tetrachlorodibenzo-p-dioxin. *Toxicology and Applied Pharmacology* **46**: 279-303, 1978.

6. Pathology Working Group. Hepatotoxicity in female Sprague-Dawley rats treated with 2,3,7,8-tetrachlorodibenzo-p-dioxin (TCDD). Prepared by R. M. Sauer, PWG Chairperson and D. Goodman, Pathco, Inc. submitted to R. A. Michaels, Chairperson, Maine Scientific Advisory Panel, April 27, 1990.
7. Maronpot, R. R., Foley, J. F., Takahashi, K., Goldsworthy, T., Clark, G., Tritscher, A., Portier, C. and Lucier, G. Dose-response for TCDD promotion of hepatocarcinogenesis in rats initiated with DEN; Histologic, biochemical and cell proliferation endpoints. *Environmental Health Perspectives* **101**, 634-642. 1993.
8. Pitot, H. Goldsworthy, T., Moron, S., Kenan, W., Glavert, H., Maronpot, R., and Campbell, H. A method to quantitate the relative initiating and promoting potencies of hepatocarcinogenic agents in their dose-response relationships to altered hepatic foci. *Carcinogenesis* **8**, 1491-1499. 1987.
9. Kohn, M., Lucier, G., Clark, G., Sewall, C., Tritscher, A. and Portier, C. A mechanistic model of the effects of dioxin on gene expression in the rat liver. *Toxicology and Applied Pharmacology*, **120**, 138-154. 1993.
10. Buchmann, A., Stinchcombe, S., Kurner, W., Hagenmaier, H. and Bock, K. Effects of 2,3,7,8-tetrachloro- and 1,2,3,4,6,7,8-heptachlorodibenzo-p-dioxin on the proliferation of preneoplastic liver cells in the rat. *Carcinogenesis* **15**, 1143-1150. 1994.
11. Portier, C. J., Tritscher, A., Kohn, M., Sewall, C., Clark, G., Edler, L., Hoel, D. and Lucier, G. Ligand-Receptor Binding for 2,3,7,8-TCDD: Implications for Risk Assessment, *Fundamental and Applied Toxicology* **20**, 48-56. 1993